Influence of Polydispersity on the Micellization of Triblock Copolymers Investigated by Pulsed Field Gradient Nuclear Magnetic Resonance

Markus Nilsson,* Björn Håkansson, Olle Söderman, and Daniel Topgaard

Physical Chemistry 1, Center for Chemistry and Chemical Engineering, Lund University, P.O. Box 124, SE-221 00 Lund, Sweden

Received June 12, 2007; Revised Manuscript Received September 4, 2007

ABSTRACT: The molecular motion in water of the poly(ethylene oxide)-poly(propylene oxide)-poly(ethylene oxide) triblock copolymer with the nominal composition $EO_{97}PO_{68}EO_{97}$ (F127) was investigated with the aid of pulsed field gradient nuclear magnetic resonance (PFG NMR). The signal decays in the PFG experiments have been recorded for 1 wt % F127 in the temperature range from 288 to 313 K and in the concentration range 0.1−35 wt % at 298 K. Below the critical micellization temperature (cmt) or the critical micellization concentration (cmc), the PFG signal decays approximately linearly when the intensities are plotted on a logarithmic scale versus the experimentally relevant parameter. At the cmt or cmc, the signal decays are curved. The NMR data were processed using inverse Laplace transformation to obtain the distribution of self-diffusion coefficients, $P(D)$. At 288 K for a 1 wt % solution, a narrow distribution was observed, while at 302 K a bimodal distribution was observed. This observation can be explained by the polydispersity of the polymer. It implies that, at a given temperature, only the more hydrophobic compound of F127 takes part in the aggregation process, while the more hydrophilic components diffuse as free nonassociated polymer. Increasing the temperature to 313 K resulted in a monomodal distribution, suggesting that all the polymers are aggregated. It is suggested that an ideal mixing model for the Pluronic micelles can explain the self-diffusion data. The NMR self-diffusion raw data were also analyzed with the COmponent REsolved (CORE; Stilbs, P.; Paulsen, K. *Rev. Sci. Instrum.* **1996**, *67*, 4380−4386) algorithm, resulting in spectra for free block copolymer and micellized block copolymer. With an increase in temperature, the intensity of the peaks for free block copolymer is reduced, whereas the intensity of the peaks for aggregated block copolymer increases. The ratios between the size of the PEO and PPO blocks (mEO/nPO) show a marked increase in free polymer compared to the ratio observed in micellized polymer when the temperature is increased. The effect of added salts to a 1 wt % F127 solution at 303 K was investigated to determine how the populations of free and micellized surfactant were changed on account of the ions present. Finally, the diffusion behavior of Pluronic F68 ($EO_{76}PO_{29}EO_{76}$) at 35 wt % has been investigated from 298 to 313 K. Both the diffusion time and the time of the gradient have been varied. The data show that the diffusion is Gaussian in the temperature range.

I. Introduction

Nonionic poly(oxyethylene)-poly(oxypropylene)-poly(oxyethylene) ($EO_xPO_yEO_x$) triblock copolymers, often called by their trade name Pluronic, self-assemble into micelles and lyotropic liquid crystalline phases. Thus, in many respects, they behave as traditional nonionic ethoxylated surfactants, C_yEO_x, with two notable differences. First, their critical micelle concentration (cmc) values are strongly sensitive to temperature. Upon changing the temperature by 20 K, the cmc can change by 3 orders of magnitude,[2] whereas the cmc shift for C_yEO_x for the same temperature change is small.[3] At constant concentration, the transition from free polymer to almost completely micellized polymer can be brought about by changing the temperature by about 20 K.[4] The micellization process of Pluronic in water is endothermic and driven by a decrease in the polarity of the EO and PO segments during the self-assembly.[2,4,5] The process is thus driven by entropy. Second, the variation of cmc with the number of PO blocks is rather weak. The energy of transfer from water to the micelle core of one PO unit is 0.25 ± 0.05 kT,[4] while the corresponding quantity for a methylene group is 1.2 kT.[6] This significant difference has an impact on the equilibrium and dynamic properties of the self-assembly of Pluronics, as compared to those of conventional nonionic surfactants. Finally, we note that, unless purification processes are carried out, Pluronics, being synthetic polymeric molecules, are polydisperse both in overall size and in the ratio of the block sizes.

Pulsed field gradient nuclear magnetic resonance (PFG NMR) is a convenient method to characterize micellization,[7] and therefore it comes as no surprise that the micellization process of different types of $EO_xPO_yEO_x$ has been investigated by PFG NMR. When micellization of conventional surfactants is studied by PFG NMR, the following events typically occur. Below the cmc, the self-diffusion of the surfactant in its nonassociated form is measured, and, for reasonably low cmc values (cmc < 50 mM or so), the self-diffusion is approximately independent of concentration. At and above the cmc, there is a continuous decrease of the surfactant self-diffusion coefficient upon further addition of surfactant because the fraction of micellized surfactant increases and the micelles diffuse slower since they are larger objects than the individual surfactant. The surfactant is well described by a single diffusion coefficient on account of the fast exchange of surfactants between the non-micellized and micellized states. In the context of PFG NMR, linear Stejskal−Tanner plots are observed (see below). The condition for fast exchange is set by the NMR time scale, which is given by the

* Corresponding author. Telephone: +46-46-222 81 50. Fax: +46-46-222 44 13. E-mail: markus.nilsson@fkem1.lu.se.

10.1021/ma071302p CCC: $37.00
Published on Web 10/20/2007

diffusion time in the PFG NMR experiment, typically 20−1000 ms.

The picture is less clear for the self-assembly of EO_xPO_y-EO_x. Fleischer,[8,9] Gille et al.,[10] and Steinbeck et al.[11] all report fast exchange of the polymers on the NMR time scale during the temperature-induced self-assembly, as evidenced by near single-exponential PFG NMR decays.

Steinbeck et al.[11] also studied the guest−host interaction of tetra(4-sulfonatophenyl) porphyrin ($TPPS_4$) with $EO_{20}PO_{70}EO_{20}$ (P123) and found slow exchange between the $TPPS_4$ at the different sites (complexes of smaller aggregates/monomer and in the micelles at the palisade layer). Walderhaug and coworkers,[12−15] on the other hand, report single-exponential PFG NMR decays below the onset of self-assembly and nonexponential decays when the self-assembly has been induced by a temperature increase for F68 ($EO_{76}PO_{29}EO_{76}$) and EO_{28}-$PO_{78}EO_{28}$ (P94). They discuss this observation in terms of anomalous diffusion in the association structures formed in the gel regime. We note that they also studied F127 ($EO_{97}PO_{68}$-EO_{97}) at higher temperature (338 K) and reported single-exponential decays.[12]

Bryskhe et al.[16] performed PFG NMR measurements on very dilute aqueous solutions of $EO_5PO_{68}EO_5$ (L121) at 283 and 298 K. The polymer signal decay was single exponential at 283 K (corresponding to the self-diffusion coefficient of nonassembled polymers), while at 298 K the signal decay was bimodal. The fast component (D_{fast}), similar in value to the one at 283 K, was assigned to "free" polymer, while the slow component (D_{slow}) was assigned to the vesicle. The occurrence of two decays in the vesicle phase was discussed in terms of slow exchange between the free and vesicle states, even on time scales of seconds. This was in turn explained by the fact that the polymer was polydisperse. Bryskhe at al.[16] argued that the two populations were chemically different. In fact, careful investigation of the decay of the slow component revealed that the polymer also exchanged slowly between different vesicle sizes.

Flodström et al.[17] studied the mechanism of the synthesis of mesoporous silica of the SBA-15 type, using P123 as structure director. They followed the structure evolution by time-resolved TEM and in situ ^{1}H NMR. With ^{1}H NMR, two overlapping methylene peaks could be resolved: one belonging to the hexagonal phase and the other to the liquid phase. As the reaction finished, they separated the top liquid phase and performed PFG NMR measurements and concluded that the batch used contained a short PO and/or EO-rich polymer fraction that was incorporated in the spherical micelles but not in the tightly packed aggregates.

Hvidt at al.[18,19] investigated the effects of polydispersity on micellization and sphere-to-rod transition of the Pluronics (P94 and $EO_{26}PO_{40}EO_{26}$ (P85)) using different liquid chromatography techniques. They found that the samples contained approximately 10−12 wt % lower size impurities. The critical micellization temperature (cmt) and sphere-to-rod transition temperatures were significantly influenced, depending on the fraction that was investigated. They also concluded that there was a distribution in composition of PO block lengths and that micelles formed at temperatures where both free polymers (low molecular weight species) and micelles (high content of PO) were present.

Of relevance is also the report that F127 may contain as much as 18% low size impurities as measured by size exclusion chromatography.[20]

Of special interest is the study by Jansson et al.[21] that used dynamic light scattering and found a broadening in the distribution of characteristic relaxation times upon micellization of F127, which was due to polydispersity in both mass and composition.

Finally, addition of inorganic salts, alcohols, and other nonelectrolytes is a common method for altering the solvent properties and changing the cmc of the nonionic polymer, for example, Pluronics. The aggregation properties of Pluronics in aqueous solutions are very sensitive to the addition of such cosolutes.[22−27] In general, with different inorganic salts, the micellization and gelation properties follow the same type of transition as the salt-free system, but all the transition temperatures are shifted. Malmsten and Lindman[25] studied the phase diagram of F127 under addition of NaCl and NaSCN and found that the cloud points were shifted to lower and higher temperatures, respectively.

Here, we report on the temperature and concentration-induced micellization of Pluronics F127 and F68, with the explicit aim to analyze the signal attenuation decay of PFG NMR raw data in detail. We discuss the effect of polydispersity on the signal decay and present simulated signal decays, which describe the experimentally observed decays. Included and discussed in this article is also the effect on the signal decay of Pluronics when different inorganic salts have been added to the system. A pervading theme of the work is an attempt to show the usefulness of PFG NMR in studying self-assembly processes.

II. Experimental Section

Materials. Two triblock polymers were used in this study. F127 has a nominal molecular weight of 12 600 g/mol. It was a kind gift from BASF, Performance Chemicals. The second polymer, F68, has a nominal molecular weight of 8350 g/mol and was obtained from Fluka, Buchs SG.

Heavy water, D_2O (99.8%), was purchased from Dr. Glaser. The following salts were used: sodium hydroxide, NaOH, 99%; sodium fluoride, NaF, 99%; sodium chloride, NaCl, 99.5%; sodium bromide, NaBr, 99.9%; sodium tiocynate, NaSCN, 98.6%; and sodium iodine, NaI anhydrous. They were all purchased from Merck.

All samples were prepared by weight, directly in 5-mm NMR test tubes. Some samples (high Pluronic concentration) were left overnight for equilibration at approximately 277 K. Where appropriate, the concentration used was 1 M for all investigated salts.

III. Methods

Self-Diffusion. PFG NMR measurements were performed on a Bruker DMX-200 MHz spectrometer or on a Varian Unity 360 MHz spectrometer equipped with field gradient probes. In the experiment, ^{1}H peaks were observed with a stimulated echo pulse sequence:[7,28−30] 90°-τ_1-90°-τ_2-90°-τ_1-echo. The gradient pulses were of duration δ and of strength g. The separation between the leading edges of the gradient pulses was $\Delta = \tau_1 + \tau_2$, and the effective diffusion time was $t = \Delta - \delta/3$.

The sample temperature was varied from 288 to 313 K, and the gradient in temperature over the sample volume was around ±0.5 K.

To minimize effects due to convection during measurements at higher temperatures, suggestions given in ref 31 were followed. Different diffusion times were used to ascertain that no influence of convection corrupted the data.

For Gaussian self-diffusion of a single species, the intensity, I, of the NMR signal decay can be written as:

$$I = \frac{I_0}{2} \exp(-2\tau_1/T_2 - \tau_2/T_1) \exp(-kD) \qquad (1)$$

where k is defined as $k \equiv \delta^2\gamma^2g^2(\Delta - \delta/3)$, I_0 is the intensity following a single 90° pulse, T_1 and T_2 are the longitudinal and transverse relaxation times, D is the self-diffusion coefficient, and γ is the magnetogyric ratio of the spin bearing nucleus. If the

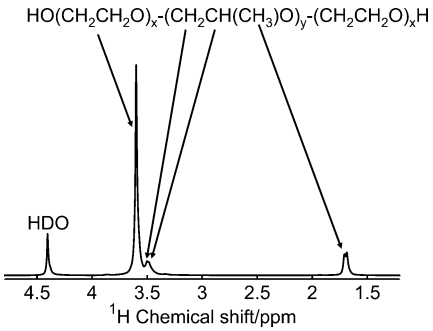

Figure 1. ^{1}H NMR spectrum of F127 at 1 wt % at 298 K in D_2O. The chemical structure of the Pluronics is included, along with the assignment of the peaks.

times τ_1 and τ_2 are kept constant, the first exponent in eq 1 is constant, and a plot I vs k yields a single-exponential decay. The representation of log(I) vs k is often referred to as a Stejskal−Tanner plot, and we shall use this term here.

The case of overlapping peaks or when there is slow exchange between the aggregated species and molecularly dispersed species will be dealt with in the section "Data Evaluation".

Relaxation. To be able to compare the areas obtained from the echo experiments for the different peaks (cf. Figure 1) properly, one needs to establish if they are relaxation weighted and compensate accordingly (cf. eq 1). Therefore, we determined the T_1 (inversion recovery experiment) and T_2 (spin echo experiment) relaxation times.

IV. Data Evaluation

Synthetic polymers are almost always polydisperse in molecular weight. This fact complicates the interpretation of NMR diffusion data from polymer systems.[32−34] Normally, one cannot separate the different components on the basis of their different chemical shifts and relaxation times, because these parameters tend to be identical. On the other hand, it is possible to separate the components using self-diffusion, because diffusion depends on size. The signal decay for a polydisperse system is given by:

$$I(k) = I_0 \int_0^\infty P(D) \exp(-kD)\, \mathrm{d}D = 1 - k\langle D\rangle + \frac{k^2}{2}\langle D^2\rangle - \ldots \quad (2)$$

where $P(D)$ is the probability density distribution of self-diffusion coefficients, and the first moment is defined as the average self-diffusion coefficient $\langle D\rangle$. In general, the functional form of $P(D)$ is not known, but it can be obtained from an inverse Laplace transformation (ILT) of $I(k)$. The ILT was performed using the Contin algorithm,[35−37] where we use an in-house written Matlab routine based on the work by Whittall and MacKay.[38]

If the functional form of $P(D)$ is known (or a functional form can be assumed), there is no reason to use the ILT. In many cases, one assumes that $P(D)$ takes the functional form of a log−normal distribution as in eq 3.

$$P(D) = \frac{1}{D\sigma_D\sqrt{2\pi}} \exp\left(-\frac{[\ln(D) - \ln(D_0)]^2}{2{\sigma_D}^2}\right) \quad (3)$$

$$\langle D\rangle = D_0 \exp\left(\frac{{\sigma_D}^2}{2}\right) \quad (4)$$

σ_D is a measure of the width of the distribution of self-diffusion coefficients. Both D_0 and σ_D can be obtained through a least-square fitting to the raw PFG NMR data when eq 3 is inserted into eq 2.

Some of the PFG NMR experimental results were analyzed with the COmponent REsolved (CORE)[1,39,40] method, introduced by Stilbs. CORE performs a global fit to all significant data points in the raw PFG NMR data set. As a consequence, the precision in the obtained parameters improves, since all the available information in the spectrum is utilized effectively. Using this approach, we have been able to deconvolute the spectra, resulting in spectra for free molecularly dispersed and for micellized Pluronics.

To obtain the distribution function in molecular weights, we use the scaling relation between the self-diffusion coefficients and the molecular weights.[32,41]

$$D = KM^{-\alpha} \quad (5)$$

where α and K are scaling parameters. The value used for α is the value for 1 wt % for poly(ethylene oxide) (PEO), $\alpha = 0.55$, given in the work of Håkansson et al.[34]

The mapping of the mass distribution onto the D distribution lacks a firm theoretical ground and therefore should be treated with some care. However, we note that the scaling relation in eq 5 rather accurately predicts the distribution of masses from diffusion data for a dilute polymer mixture with known molecular weights (see Håkansson et al.)[34] See also discussion in refs 42 and 43.

V. Results and Discussion

Introduction. The PFG NMR signal decays from Pluronics in aqueous solutions are often curved when plotted in a Stejskal−Tanner representation.[44] The curved decays could clearly by caused by several factors and mechanisms. One obvious reason is that the polymer is polydisperse in both composition and molecular weight, although we note that only polymers having relatively high polydispersity indices give rise to curved Stejskal−Tanner plots, as discussed by Fleischer.[32]

In general, our feeling is that scientists in the field do not always appreciate that Pluronics are polydisperse and misinterpretations can be found in the literature. Our aim is to discuss, highlight, and explain the appearance of Pluronic signal decays in detail, and to achieve this we use accurate data from two Pluronics: F68 and F127. For the former, we present PFG NMR signal decays at four temperatures and for the latter at six temperatures, where at each temperature we have used four different diffusion times. For F127, we also investigate the concentration dependence at 298 K. Finally, we show the effect of some different inorganic salts on the PFG NMR signal decays.

For reference, we show the proton spectrum of 1 wt % F127 at 298 K in Figure 1, with the assignment of the different peaks included.

Temperature-Induced Micellization of F127 at 1 wt %. All results and data analysis in this article are based on the intensities of the EO peak, except when otherwise stated. In Figure 2A, we display signal decays from a 1 wt % F127 aqueous solution at six temperatures. The lines in Figure 2A (except the dotted line) are predictions from the ILT process. The normalized signal decay at 288 K is to a good approximation single exponential (as given by the dotted line in the figure), although it does deviate slightly at high k values (see further below). At the other investigated temperatures, the signal decays are curved, more so for the intermediate temperatures. In thetemperature interval investigated, the polymers go from being

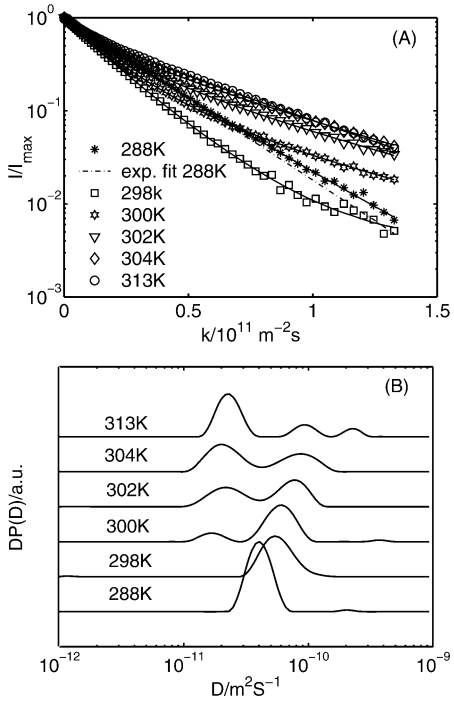

Figure 2. (A) I/I_{max} versus k for F127 at 1 wt % at various temperatures. The solid lines are the results of ILT processing. The dotted line is an exponential fit to the data set at 288 K. (B) $DP(D)$, from the ILT versus D.

dominantly molecularly dispersed as free polymer (288 K) to being associated into aggregates. At 313 K, a majority of the polymer is micellized, which explains why the signal decay again approaches that of a straight line at this temperature.

To further analyze the data, we turn to the ILT approach, which, when applied to the signal attenuation PFG NMR raw data, offers the possibility to extract the probability density distribution in self-diffusion coefficients. In Figure 2B, the results of such a procedure are plotted. At low temperatures (288 K), the obtained distribution is relatively narrow, but upon increasing the temperature, the distribution becomes wider, until at 300 K a second peak emerges. We will later suggest that these two peaks originate from free and micellized polymer, respectively. Increasing the temperature further, the peak corresponding to the slow polymer component (the aggregated polymer) is growing at the expense of the peak for the fast polymer component (free polymer). At 302 and 304 K, the peaks are approximately equal in area, indicating that roughly half of the polymer is aggregated here. At 313 K, the peak corresponding to the aggregate dominates (please note that the third peak to the right is an artifact caused by the ILT procedure). The approach used here is similar to the one normally used when interpreting dynamic light scattering data (see ref 21 for a light scattering study of the same system under the same conditions).

Figure 3 shows a plot of the normalized signal attenuation versus k for different diffusion times for 1 wt % F127 at 302 K. The condensation of the data onto one master curve indicates that there is no molecular exchange occurring with time constant in the window from 20 to 1000 ms. The slight scatter in the data points at high k values is due to poor signal-to-noise at these high k values.

We summarize the findings thus far. A 1 wt % aqueous solution of our batch of F127 undergoes a temperature-induced micellization process over a range of roughly 20 K. During this process, the PFG NMR decays are nonlinear in a Stejskal−Tanner plot. The ILT procedure indicates that there are two

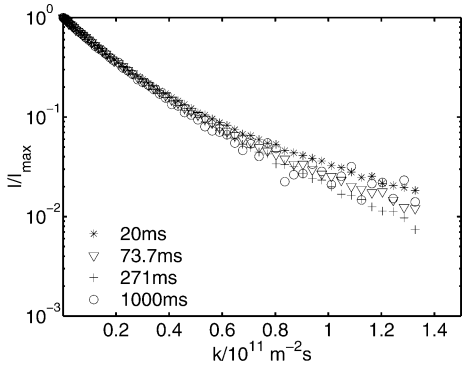

Figure 3. I/I_{max} versus k for 1 wt % F127 at 302 K using four different diffusion times: 20, 73.7, 271, and 1000 ms.

populations of polymers with different diffusion coefficients in the range where micellization occurs. The lack of dependence on the diffusion time indicates that there is no exchange between the populations occurring during the investigated range of diffusion times.

The next step is to explain the appearance of the signal decays. We start by referring to the fact noted earlier that the signal decay at 288 K, where the polymer is almost exclusively in the free form (no micelles are formed at this temperature), does show a minor deviation from single-exponential decay (Figures 2A and 4A). We have analyzed this by assuming a log−normal distribution of self-diffusion coefficients, using a nonlinear least-square fit to the data, using eq 2 with eq 3 inserted.

The obtained average self-diffusion coefficient is $\langle D \rangle = 4.31 \times 10^{-11}$ m^2 s^{-1} obtained from eq 4 ($D_0 = 4.19 \times 10^{-11}$ m^2 s^{-1} and $\sigma_D = 0.24$). The result of the different fitting approaches—exponential fitting (eq 1), log−normal distribution (eq 3 inserted into eq 2), and Contin—is displayed in Figure 4A. In Figure 4B, $DP(D)$, from the log−normal and ILT procedures is shown. $DP(D)$ obtained from the two approaches overlaps smoothly.

The obtained $P(D)$ can be used to calculate the distribution in molecular weight, $P(M)$, using appropriate scaling relations.[32,34,41] Here, we use the one given in eq 5, with values of the scaling parameters ($\alpha = 0.55$) taken from PFG NMR data for 1 wt % PEO at 298 K.[34] The resulting molecular weight distribution, $P(M)$, as converted from $P(D)$ using procedures described in ref 34, is given in Figure 5 together with the result of a non-linear least-square fit of a log−normal distribution in molecular weight (eqs 3 and 4 with D replaced by M). The obtained average molecular weight is ($\langle M \rangle = 11 \times 10^3$ g/mol, $M_0 = 10 \times 10^3$ g/mol, $\sigma_M = 0.43$). A value of $\sigma_M = 0.43$ indicates that the polymer is rather polydisperse with a polydispersity index of 1.2. We stress that the effects on the signal decay is rather moderate; this corroborates the conclusion of Fleischer,[32] that rather large polydispersity is needed to induce sizable deviations from single-exponential decays.

Thus, we have shown that the F127 sample is considerably polydisperse in molecular weight. Matters are further complicated by the fact that a Pluronic can be polydisperse in properties at constant molecular weight through a variation in the ratio of the block sizes.

We proceed to model the signal intensity decays of the aqueous solution of F127 polymer with a multicomponent ideal mixture model that is based on the phase separation model.[45] The model consists of the following steps. We use the distribution of molecular weights presented in Figure 5 and assume that the individual cmc value for each polymer component depends logarithmically on the molecular weight

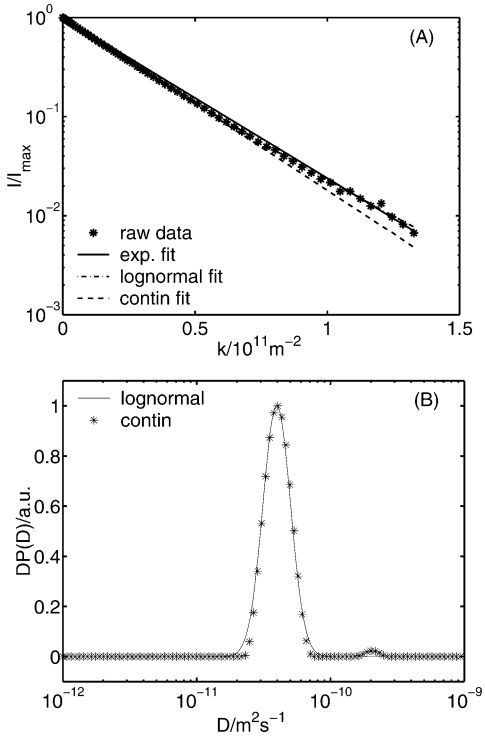

Figure 4. (A) I/I_{max} versus k for F127 at 1 wt % at 288 K. Included are also predictions of an exponential fit, a log−normal distribution fit, and a Contin treatment. (B) Obtained $DP(D)$ from the ILT approach and from the fit of a log−normal probability density distribution versus D.

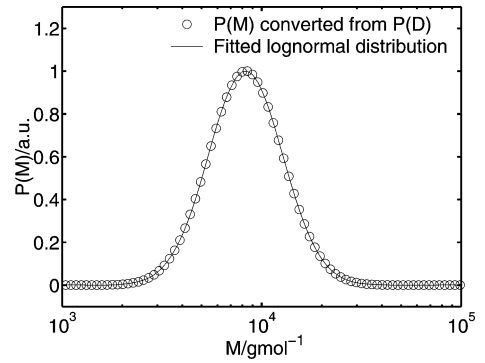

Figure 5. $P(M)$ from the transformation of $P(D)$ (Figure 4) versus M. Also included is a fit to a log−normal $P(M)$.

in analogy with the case of C_yEO_x surfactants where cmc values decrease logarithmically with the number of carbons in the tail of the surfactant.[3] This allows us to calculate a distribution of cmc values as well as the effective cmc value for the mixture using results from ref 45. Finally, we generate the fraction-free and micellized of each polymer component, again using results from ref 45.

We then assume that all the polymer components of the polydisperse mixture exchange rapidly on the NMR time scale, but the fraction-free polymer, P_{free}, varies depending on the assigned cmc value. For each polymer component, we write a two-site exchange equation for the observed diffusion coefficient.

$$D_{obs} = D_{free}(P_{free}) + D_{mic}(1 - P_{free}) \quad (6)$$

where D_{free} and D_{mic} are the diffusion coefficient of the free polymer and of the micelle, respectively. Please note that we assume only two diffusion coefficients (eq 6); this is an approximation on account of the polydisperse nature of the polymer, but it is probably a reasonable approximation, since the signal decays are to a good approximation single exponential below and above the cmt (Figure 2A). Finally, signal decay is synthesized by summing signal decays from each polymer component with suitable weighing factors. The result is presented in Figure 6A, and the ILT of the model decay is given in Figure 6B. Clearly, the model accounts for the experimentally obtained decays reasonably well.

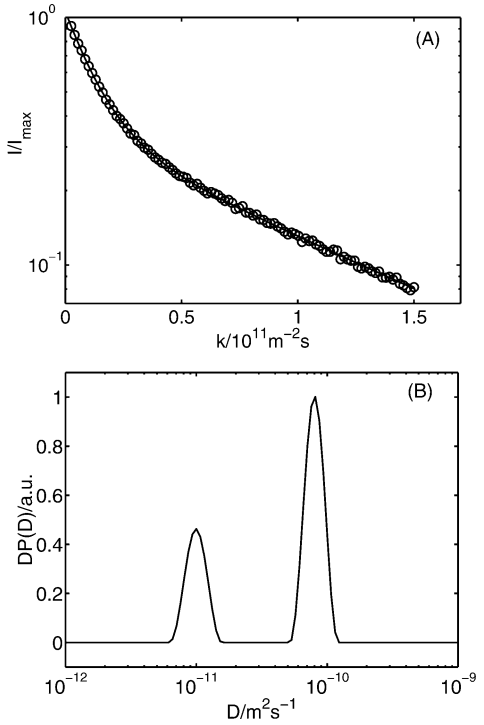

Figure 6. (A) Generated signal attenuation, I/I_{max} versus k. Noise has been added to the data set. Values for D_{slow} and D_{fast} are 1×10^{-11} and 8×10^{-11} m^2 s^{-1}, respectively. (B) $DP(D)$ from the ILT performed on the generated signal attenuation versus D.

The physics underlying the behavior is that only a minute fraction of the polymer components have cmc values around the effective cmc (and thus would have a diffusion coefficient intermediate between D_{free} and D_{mic}), while others are almost completely bound or free. The hydrophilic polymer components remain in solution and take little part in the association process, while the more hydrophobic polymers are to a large extent micellized at the given temperature and concentration.

The fact that we can write the observed signal decays in terms of two diffusion coefficients is important for it allows us to calculate some important characteristics of the association process.

First, we determine the hydrodynamic radii, R_H, of the free polymer and of the micelles as a function of temperature. A global fitting procedure (using eq 1 for 288 K and eq 2 for the other temperatures) involving four diffusion times and a total of 256 data points was used to obtain D_{free} and D_{mic} at each temperature. The Stokes−Einstein relation is used to calculate R_H.

$$D = \frac{k_B T}{6\pi\eta R_H} \quad (7)$$

where k_B is the Boltzmann constant, η is the viscosity of the solvent (D_2O), and T the absolute temperature.

In Figure 7, the hydrodynamic radii have been plotted for the free and micellized polymers. The size of the micelles

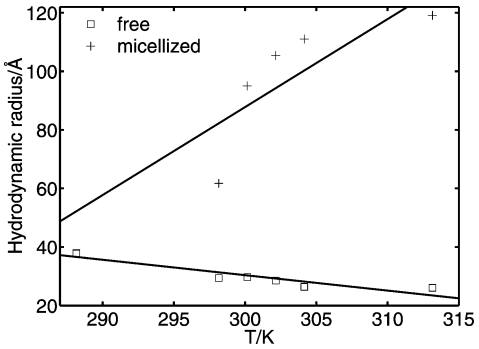

Figure 7. R_H versus T, for micellized and free polymers for 1 wt % F127 polymer solution. The lines are guides for the eyes.

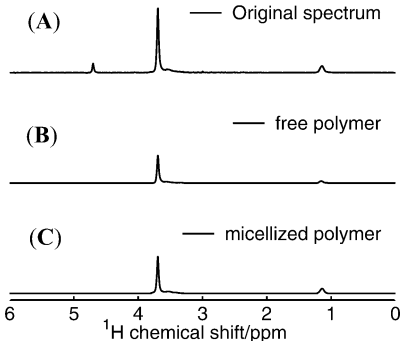

Figure 8. CORE approach[1,39,40] has been applied to separate overlapping peaks for F127 at 1 wt % at 302 K.

increases from approximately 40 Å to 120 Å. This is in line with results from other techniques: small-angle neutron scattering,[4,46] dynamic light scattering,[21] and fluorescence quenching.[47] Mean field lattice calculations[48,49] also indicate that the aggregation number increases with increasing temperature.

There is a small but significant decrease in size for the free polymers as the temperature is increased. Two reasons account for this. First, and probably foremost, it is polymer components with smaller molecular weights that remain free as the temperature is increased. Second, as the temperature is increased, dehydration of the EO parts occurs, leading to an effectively smaller size of the diffusing species.

The second characteristics that can be obtained from the data are the evolution of the ratio of the block sizes, quantified as the ratio of number of EO units to number of PO units. To obtain this quantity, we will use the CORE approach to deconvolute the spectra on the basis of the difference in diffusion coefficients.

In Figure 8, an example of the CORE approach of 1 wt % F127 at 302 K is shown. The three spectra in the figure are the original spectrum (A), the spectrum of the free polymer corresponding to D_{fast} (B), and finally, the spectrum of the slow component corresponding to D_{slow} (micellized polymer) (C). The results from the CORE analysis have been further analyzed by integrating the peaks in the spectrum (see Figure 1 for the proton spectrum and labeling of peaks). Before integrating the peaks, one needs to make suitable corrections for relaxation weighting so the areas given in the spectrum can be compared properly. Recall that we are using spin echo experiment to generate the NMR spectra (eq 1). T_1 and T_2 relaxation measurements were performed, and the relaxation-dependent terms (cf. eq 1) were calculated and used in the data treatment. We note that these terms in all cases were close to unity.

The ratio between the number of the EO units and PO units for the free, micellized, and total (the latter is included as a control) as calculated from the deconvoluted spectra produced by the CORE approach is presented in Figure 9. This gives us further quantitative valuable insight into the temperature-induced association process of F127. Focusing on the ratio for the micellized F127, we find that the ratio increases mildly as a function of temperature, indicating that at low temperature the more hydrophobic polymer components of F127 take part in the association, while the polymer components with larger ratios of EO to PO do not take part in the association.

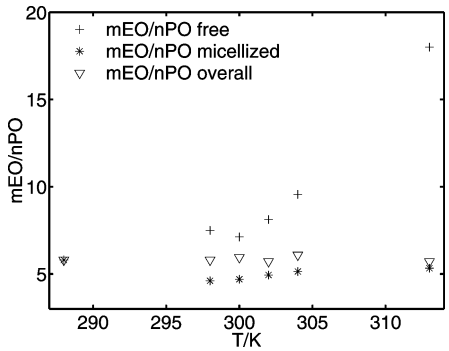

Figure 9. Ratio between the numbers of EO units (m) to PO units (n) versus T. The cases of free, micellized, and overall are shown (see text for details).

Turning to the ratio between EO to PO for the free polymer, we find that the ratio also increases, but the increase is considerably more pronounced. At the highest temperature investigated, the remaining free polymer component is very rich in EO units.

In summary, the curved Stejskal−Tanner plots obtained while passing though the micellization at 1 wt % of F127 are due to the polydispersity of the polymer. A multicomponent ideal mixture model can explain the appearance of the curves, and there is no need to invoke slow exchange of polymers or anomalous diffusion. In fact, one of the strengths of the PFG NMR technique is that it enables one to judge whether a diffusion process is Gaussian or not. This will be the topic of the next section.

Temperature-Induced Micellization of F68 at 35 wt %. In this section, we consider the temperature-induced micellization of F68 at 35 wt %. A similar study was previously presented by Walderhaug and Nyström,[14] who discuss their results in terms of anomalous diffusion where the mean squared displacement scales with time with a scaling parameter less than 1 ($\langle Z^2 \rangle = t^r$; $r < 1$). Here, we show how PFG NMR can be used to determine whether the diffusion is Gaussian or not.

Phase diagrams of F68 have been determined by Wanka et al.[4] and Wu et al.[27] On increasing the concentration of F68 at 298 K, we find that the phase diagram shows an isotropic phase up to approximately 47 wt % (the cmc is around 35 wt %), and then there is a narrow two-phase area with micellar and cubic phase in equilibrium. The cubic phase consists of discrete packed micelles.[46,50]

A sample at 35 wt % was investigated with PFG NMR in the temperature range from 298 to 313 K. According to the phase diagram, in this range micelles are formed. In Figure 10, the PFG NMR signal decays for four different diffusion times (50, 100, 200, and 400 ms) at four different temperatures (298, 303, 309, and 313 K) versus k are shown. Each graph contains 12 different data sets: for each of the four different diffusion times, three different gradient pulse lengths have been used (3, 10, and 20 ms). The gradient amplitude is then adjusted so that the same window of k values is covered in each curve. The main conclusion drawn from Figure 10 is that the 12 curves

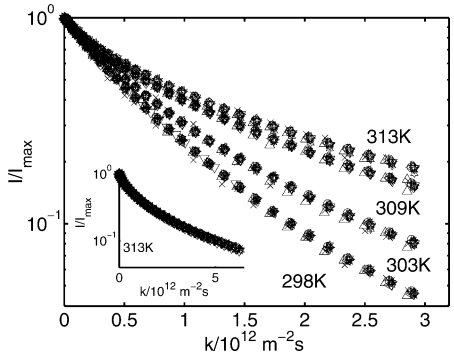

Figure 10. I/I_{max} versus k, for Pluronic F68 at 35 wt % at different temperatures. For each temperature, four different diffusion times $\Delta = 50$, 100, 200, and 400 ms and three different $\delta = 3$, 10, and 20 ms were used. The inset shows measurements at 313 K with different settings $\Delta = 60$, 120, 180, and 420 ms and $\delta = 4$, 10, and 20 ms.

for each temperature fall onto a common master curve, implying that the diffusion is Gaussian.[51]

To appreciate this, we have to digress slightly and discuss the theory underlying eq 1. Equation 1 (and consequently eq 2) is only valid for Gaussian diffusion. This can be seen in the following way. When introducing the quantity k, we are effectively stating that it is only the area (i.e., the product δG) under the gradient pulse that determines the signal decay. However, for non-Gaussian diffusion, this is no longer true, and the echo decay will in fact depend on the value of δ for the same value of k. Now, curvature in Stejskal−Tanner plots can be caused by many reasons. Non-Gaussian or anomalous diffusion is one reason; a distribution of diffusion coefficients as described by eq 3 is another. But it is only for the latter case that the echo decays are independent of the value of the gradient pulse length. As is evident from Figure 10, this is in fact the case of the decays from F68. Thus, the curvature in the Stejskal−Tanner plots is caused by polydispersity in the material, and there is no reason to invoke anomalous diffusion to rationalize the curvature.

Concentration-Induced Micellization. The F127 self-diffusion was also studied as a function of concentration at constant temperature, covering the range in concentrations from below the cmc to above the cmc. The F127 PFG NMR signal decays will again be in focus. We start by reviewing the phase diagram.[4] At 298 K, the phase diagram has an isotropic phase up to approximately 18 wt %, and then there is a narrow two-phase area with micellar and cubic phases in equilibrium. Finally, at approximately 85 wt %, crystals of F127 start to form. The cubic phase consists of discrete micelles, packed on a cubic lattice. Before going into the results, it should be mentioned that Malmsten and Lindman[25] have performed related but less detailed studies with self-diffusion NMR on F127, and they report that the exchange process of Pluronics between the free and micellized states was slow (on the order of hours).

At 0.1 wt % F127, the signal decay is approximately single exponential, whereas at 1 wt % the signal decay is slightly curved (Figure 11A). The cmc at 298 K is approximately 0.7 wt % (0.555 mM),[2] in line with this observation. At 5, 10 (Figure 11B), and 15 wt % (Figure 11C), the F127 signal decays are highly curved, but the curvature and in particular the crossover from a large to low slope are different. With reference to the earlier discussion, this signals a change in the fraction of free polymer as the concentration is increased. A difference to the temperature-induced micellization is that the diffusion of the micelles becomes progressively slower as the volume fraction

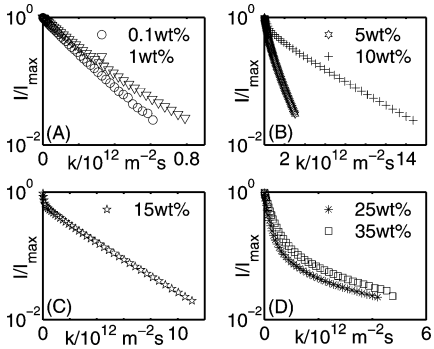

Figure 11. I/I_{max} versus k for F127 at different concentrations (0.1−35 wt %) at 298 K. These data were obtained using a Hahn echo sequence.

of micelles increases (at the much higher volume fractions in the latter case) on account of obstruction effects.[7,52]

At 25 and 35 wt % (Figure 11D) in the cubic phase, the curvature is still very pronounced but the general appearance of the curves are different from the one for 15 wt %. The diffusion process in the cubic phase is different from that in the micellar phase.[53,54] In the former, the micelles are stationary and the diffusion takes place through random walk of polymers between micelles in the cubic lattice. This "walk" is mediated through the bulk solution. Again, it is the fractionation of the polymer into the micelles on the basis of its hydrophobicity that gives rise to the variation in the mean square displacements underlying the curved signal decays. Finally, we note that there may be a complication in the cubic phase because of the complicated relaxation in such phases.[55]

Effects of Salts on the Micellization. To further show the usefulness of PFG NMR in the study of self-assembly of Pluronics, or indeed of any self-assembling system, we have investigated the effect of different inorganic salts on the association in a 1 wt % F127 solution at 298 K. The influence of simple salts on colloidal aggregates is a central topic in colloidal science. Ions are commonly ordered with respect to their effects in Hofmeister series, originally introduced to describe the propensity of ions to precipitate proteins from aqueous solutions. Recently, there has been a renewed interest in these series, and some progress has been made toward explaining in a general sense the origin of the effects. Often, the effects are ascribed to the influence the ions have on the water structure (terms such as "structure-breaking" or "structure-making" ions are often used), but a better alternative is to describe the effects of salts in terms of their affinities (or lack of) to surfaces.[6]

Effects of various ionic additives on Pluronic systems have been the subject of many studies.[22,24−26,56−58] Salt addition to F127 system has been studied by Su et al.[26] by Fourier transformation infrared spectroscopy. They found that the cmt is significantly modified, and they argued that this was caused by the salt changing the solubility of the PO part.

In Figure 12A, the normalized signal decay is plotted versus k for F127 solutions with six different salts, at a concentration of 1 M at 303 K. As a reference, the curve for the salt-free case is also given. As can be seen, the curves from the samples with the so-called "salting-in" salts (NaI and NaSCN) decay faster than the decay of the reference F127, giving indication of a faster self-diffusion coefficient, which is caused by an increased fraction of free polymer, induced by the addition of the salts. On the other hand, the "salting-out" salts (NaF, NaOH) give rise to slower decays then the reference, indicating that a larger fraction is in the micellized state in comparison to F127 alone.

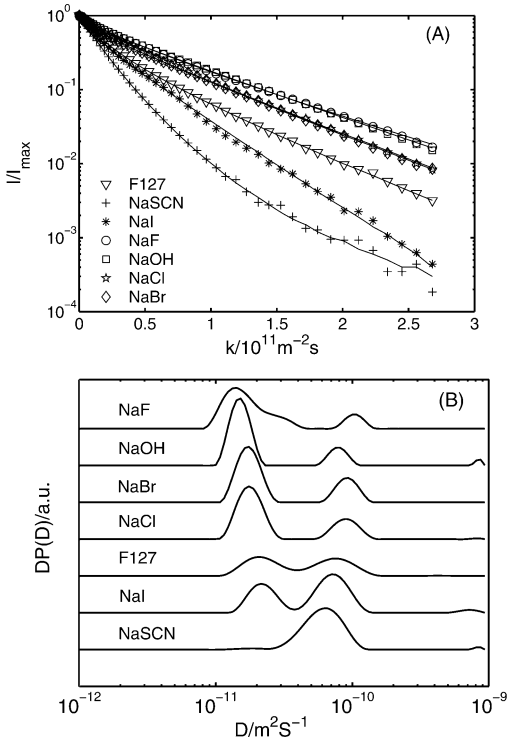

Figure 12. (A) I/I_{max} versus k, for 1 wt % F127 at 303 K for six different sodium salts at a concentration of 1 M. Included is the decay of a salt-free F127 solution. (B) $DP(D)$ versus D from the data in part A.

A clearer view of the salts' effect on the micellization is given in Figure 12B, where ILT of the signal decays in Figure 12A are presented. Figure 12B clearly shows that the "salting-out" salts favor micellization, while the "salting-in" salts destabilize the micelles. The trends in Figure 12B follow the typical Hofmeister series.

The effect of the different "salting-in" ions on the signal decay can be explained by the fact that the ions are relative large and polarizable, and hence have some affinity to the polymer surface relative to the bulk, making the polymer partially charged, which increases the solubility of the polymers and also the cloud point.[23]

The "salting-out" salts have on the other hand no affinity for the polymer surface and instead show depletion around the polymer. The "salting-out" salts increase the polarity of the solvent and thereby decrease the solubility and cloud point of the polymer. The effect affects the signal decay, which decays slower due to the salt-induced aggregate formation.

VI. Conclusions

In the present work, we investigate the micellization of Pluronic F127 as a function of temperature, concentration, and inorganic salt addition by ^{1}H self-diffusion NMR.

The distribution of self-diffusion coefficients of an aqueous solution of 1 wt % F127 changes significantly upon changing the temperature. At intermediate temperature, the signal decay is highly curved, indicating a broad distribution of self-diffusion coefficients. In the literature, the observation is often discussed in terms of slow exchange between polymer in the micelles and the free polymer in solution. Here, we argue that this behavior is due to the polydispersity of the polymer in both molecular weight and chemical composition (see also ref 14). This results in a fractionation of the polymer; the hydrophobic compound is primarily associated with micelles while the opposite is true for the more hydrophilic components. Each component is in fast exchange on the NMR time scale. We have quantified the self-assembly of Pluronics molecularly by determining the EO/PO balance in the micelles and free polymers. With increasing temperature, the ratio for the free polymer increases, meaning that the polymers that remain in solution tend to be more and more hydrophilic. On the other hand, the ratio for the polymers in the micelle increases slightly.

We have modeled the curved NMR signal decays using a model based on ideal solution theory.

The concentration-induced micellization displays curved signal decays at intermediate and high concentrations which are also due to the polymer polydispersity.

On addition of 1 M inorganic salt to a 1 wt % solution of F127 at 303 K, a substantial influence on the signal decays was observed in comparison to a solution of F127 alone. The "salting-in" salts (NaI and NaSCN) decay faster than the decay of the reference F127. The "salting-out" salts (NaF and NaOH) favor micellization, giving a slower decay in comparison to the reference F127. By using different salts, one can tune the distributions of self-diffusion coefficients, as is also possible by varying the temperature or concentration.

We analyze the temperature-induced micellization of Pluronic F68 at 35 wt %.[14] The signal decay is highly curved, which we argued is because F68 is polydisperse.

Finally, we stress that it is important to always consider polydispersity when interpreting any data concerned with the self-assembly of polymer material, in particular in the context of exchange rates between aggregated and nonaggregated states.

Acknowledgment. O.S. and D.T. thank the Swedish Research Council (VR) for financial support.

References and Notes

(1) Stilbs, P.; Paulsen, K. *Rev. Sci. Instrum.* **1996**, *67*, 4380−4386.
(2) Alexandridis, P.; Holzwarth, J. F.; Hatton, T. A. *Macromolecules* **1994**, *27*, 2414−2425.
(3) Holmberg, K.; Jönsson, B.; Kronberg, B.; Lindman, B. *Surfactants and polymers in aqueous solution*, 2 ed.; Wiley & Sons: Hoboken, NJ, 2003.
(4) Wanka, G.; Hoffmann, H.; Ulbricht, W. *Macromolecules* **1994**, *27*, 4145−4159.
(5) Alexandridis, P.; Hatton, T. A. *Colloids Surf.* **1995**, *96*, 1−46.
(6) Evans, D. F.; Wennerström, H. *The colloidal domain: where physics chemistry, biology, and technology meet*, 2 ed.; Wiley-VCH: New York, 1999.
(7) Söderman, O.; Stilbs, P. *Prog. Nucl. Magn. Reson. Spectrosc.* **1994**, *26*, 445−482.
(8) Fleischer, G. *J. Phys. Chem.* **1993**, *97*, 517−521.
(9) Fleischer, G.; Blob, P. *Colloid Polym. Sci.* **1993**, *271*, 217−222.
(10) Gille, K.; Knoll, H.; Rittig, F.; Fleischer, G.; Kärger, J. *Langmuir* **1999**, *15*, 1059−1066.
(11) Steinbeck, C. A.; Hedin, N.; Chmelka, B. F. *Langmuir* **2004**, *20*, 10399−10412.
(12) Walderhaug, H. *J. Phys. Chem. B* **1999**, *103*, 3352−3357.
(13) Walderhaug, H. A PFG NMR Study of Polymer Diffusion in Aqueous Systems of Some Poloxamers. In *Slow Dynamics in Complex Systems;* 8th Tohwa University International Symposium, Fukuoka, Japan, Nov 1998; Tokuyama, M., Oppenheim, I., Eds.; AIP Conference Proceedings 469; American Institute of Physics: Woodbury, NY, 1999; pp 136−137.
(14) Walderhaug, H.; Nyström, B. *J. Phys. Chem. B* **1997**, *9*, 1524−1528.
(15) Walderhaug, H.; Nyström, B. *Trends Phys. Chem.* **1997**, *6*, 89−106.
(16) Bryskhe, K.; Jansson, J.; Topgaard, D.; Schillén, K.; Olsson, U. *J. Phys. Chem. B* **2004**, *108*, 9710−9719.
(17) Flodström, K.; Wennerström, H.; Alfredsson, V. *Langmuir* **2004**, *20*, 680−688.
(18) Batsberg, W.; Ndoni, S.; Trandum, C.; Hvidt, S. *Macromolecules* **2004**, *37*, 2965−2971.
(19) Hvidt, S.; Trandum, C.; Batsberg, W. *J. Colloid Interface Sci.* **2002**, *250*, 243−250.
(20) Yu, G.; Deng, Y.; Dalton, S.; Wang, Q.; Attwood, A.; Price, C.; Booth, C. *J. Chem. Soc., Faraday Trans.* **1992**, *88*, 2537−2544.

(21) Jansson, J.; Schillén, K.; Olofsson, G.; da Silva, R. C.; Watson, L. *J. Phys. Chem. B* **2004**, *108*, 82−92.
(22) Alexandridis, P.; Athanassiou, V.; Hatton, T. A. *Langmuir* **1995**, *11*, 2442−2450.
(23) Alexandridis, P.; Holzwarth, J. F. *Langmuir* **1997**, *13*, 6074−6082.
(24) Jörgensen, E. B.; Hvidt, S.; Brown, W.; Schillén, K. *Macromolecules* **1997**, *30*, 2355−2364.
(25) Malmsten, M.; Lindman, B. *Macromolecules* **1992**, *25*, 5440−5445.
(26) Su, Y.; Liu, H.; Wang, J.; Chen, J. *Langmuir* **2002**, *18*, 865−871.
(27) Wu, Y. L.; Sprik, R.; Poon, W. C. K.; Eiser, E. *J. Phys.: Condens. Matter* **2006**, *18*, 4461−4470.
(28) Kimmich, R. *NMR: Tomography, Diffusometry, Relaxometry;* Springer-Verlage: Berlin, 1997.
(29) Price, S. W. *Concepts Magn. Reson.* **1997**, *9*, 299−336.
(30) Stilbs, P. *Prog. Nucl. Magn. Reson. Spectrosc.* **1987**, *19*, 1−45.
(31) Hedin, N.; Yu, T. Y.; Furo, I. *Langmuir* **2000**, *16*, 7548−7550.
(32) Fleischer, G. *Polymer* **1985**, *26*, 1677−1682.
(33) Griffiths, P. C.; Cheung, A. Y. F.; Davies, J. A.; Paul, A.; Tipples, C. N.; Winnington, A. L. *Magn. Reson. Chem.* **2002**, *40*, 40−50.
(34) Håkansson, B.; Nydén, M.; Söderman, O. *Colloid Polym. Sci.* **2000**, *278*, 399−405.
(35) Johnson, C. S., Jr. *Prog. Nucl. Magn. Reson. Spectrosc.* **1999**, *34*, 203−256.
(36) Morris, K. F.; Johnson, C. S., Jr. *J. Am. Chem. Soc.* **1993**, *114*, 3139−3142.
(37) Provencher, S. W. *Comput. Phys. Commun.* **1982**, *27*, 229−242.
(38) Whittall, K. P.; MacKay, A. L. *J. Magn. Reson.* **1989**, *84*, 134−152.
(39) Stilbs, P. *J. Magn. Reson.* **1998**, *135*, 236−241.
(40) Stilbs, P.; Paulsen, K.; Griffiths, P. C. *J. Phys. Chem.* **1996**, *100*, 8180−8189.
(41) Chen, A.; Wu, D.; Johnson, C. S., Jr. *J. Am. Chem. Soc.* **1995**, *117*, 7965−7970.
(42) Callaghan, P. T.; Pinder, D. N. *Macromolecules* **1981**, *14*, 1334−1340.
(43) von Meerwall, E.; Palunas, P. *J. Polym. Sci., Part B: Polym. Phys.* **1987**, *25*, 1439−1455.
(44) Stejskal, E. O.; Tanner, J. E. *J. Chem. Phys.* **1965**, *42*, 288−292.
(45) Holland, P. M.; Rubingh, D. N. *J. Phys. Chem.* **1983**, *87*, 1984−1990.
(46) Wanka, G.; Hoffmann, H.; Ulbricht, W. *Colloid Polym. Sci.* **1990**, *268*, 101−117.
(47) Almgren, M.; van Stam, J.; Lindblad, C.; Li, P.; Stilbs, P.; Bahadur, P. *J. Phys. Chem.* **1991**, *95*, 5677−5684.
(48) Linse, P. *Macromolecules* **1993**, *26*, 4437−4449.
(49) Linse, P.; Malmsten, M. *Macromolecules* **1992**, *25*, 5434−5439.
(50) Mortensen, K.; Wyn, B. *Macromolecules* **1993**, *26*, 4128−4135.
(51) Malmborg, C.; Topgaard, D.; Söderman, O. *J. Magn. Reson.* **2004**, *169*, 85−91.
(52) Medina-Noyola, M. *Phys. Rev. Lett.* **1988**, *60*, 2705−2708.
(53) Bull, T.; Lindman, B. *Mol. Cryst. Liq. Cryst.* **1974**, *28*, 155−160.
(54) Svensson, A.; Topgaard, D.; Piculell, L.; Söderman, O. *J. Phys. Chem. B* **2003**, *107*, 13241−13250.
(55) Söderman, O.; Walderhaug, H.; Henriksson, U.; Stilbs, P. *J. Phys. Chem.* **1985**, *89*, 3693−3701.
(56) Hamley, I. W. *Physics of Block Copolymers;* Oxford University Press: Oxford, 1998.
(57) Panday, K.; Lad, K.; Bahadur, P. *Pure Appl. Chem.* **1993**, *A30*, 1−18.
(58) Ma, J.-h.; Guo, C.; Tang, Y.-l.; Wang, J.; Zheng, L.; Liang, X.-f.; Chen, S.; Liu, H.-z. *Langmuir* **2007**, *23*, 3075−3083.

MA071302P